



NIH Public Access

Author Manuscript

Cancer Prev Res (Phila). Author manuscript; available in PMC 2014 July 01.

Published in final edited form as:

Cancer Prev Res (Phila). 2013 July ; 6(7): 625–633. doi:10.1158/1940-6207.CAPR-13-0053.

Grape Seed Extract Efficacy against Azoxymethane-induced Colon Tumorigenesis in A/J Mice: Interlinking miRNA with Cytokine Signaling and Inflammation

Molly Derry¹, Komal Raina¹, Velmurugan Balaiya^{1,*}, Anil K. Jain^{1,*}, Sangeeta Shrotriya¹, Kendra M. Huber², Natalie. J. Serkova^{2,3}, Rajesh Agarwal^{1,3}, and Chapla Agarwal^{1,3}

¹Department of Pharmaceutical Sciences, Skaggs School of Pharmacy, University of Colorado Anschutz Medical Campus, Aurora, CO

²Department of Anesthesiology, University of Colorado Anschutz Medical Campus, Aurora, CO

³University of Colorado Cancer Center, University of Colorado Anschutz Medical Campus, Aurora, CO

Abstract

Colorectal cancer (CRC) is the second leading cause of cancer-associated deaths, suggesting that additional strategies are needed to prevent/control this malignancy. Since CRC growth and progression involve a large window (10-15 years), chemopreventive intervention could be a practical/translational strategy. Azoxymethane (AOM)-induced colon tumorigenesis in mice resembles human CRC in terms of progression of ACF to polyps, adenoma and carcinomas, and associated molecular mechanisms. Accordingly, herein we investigated grape seed extract (GSE) efficacy against AOM-induced colon tumorigenesis in A/J mice. GSE was fed in diet at 0.25% or 0.5% (w/w) dose starting two-weeks after last AOM injection for 18 or 28 weeks. Our results showed that GSE feeding significantly decreases colon tumor multiplicity and overall tumor size. In biomarker analysis, GSE showed significant anti-proliferative and pro-apoptotic activities. Detailed mechanistic studies highlighted that GSE strongly modulates cytokines/interleukins and miRNA expression profiles as well as miRNA processing machinery associated with alterations in NF-κB, β-catenin and MAPK signaling. Additional studies using immunohistochemical analyses found that indeed GSE inhibits NF-κB activation and decreases the expression of its downstream targets (COX-2, iNOS, VEGF) related to inflammatory signaling, down-regulates β-catenin signaling and decreases its target gene C-myc, and reduces phosphorylated ERK1/2 levels. Together, these finding suggested that inflammation, proliferation and apoptosis are targeted by GSE to prevent CRC. In summary, this study for the first time shows alterations in the expression of miRNAs and cytokines by GSE in its efficacy against AOM-induced colon tumorigenesis in A/J mouse sporadic CRC model, supporting its translational potential in CRC chemoprevention.

Keywords

colorectal cancer; chemoprevention; grape seed extract; inflammation; apoptosis

Requests for reprints: Chapla Agarwal; Chapla.Agarwal@ucdenver.edu. *These authors contributed equally to this work..

Disclosure of potential conflicts of interest: No potential conflicts of interest were identified by any authors of this manuscript.

Introduction

Colorectal cancer (CRC) is the second leading (both genders combined) cause of cancer-related deaths, and the third most frequently diagnosed malignancy in the United States (1). Adoption of western and sedentary lifestyles increase CRC incidence world-wide, with most (~75%) of CRC developing sporadically (2). Despite efforts, compliance with screening recommendations is low and not enough to halt cancer growth/progression and prevent associated mortality (2). Traditional CRC chemopreventive agents, such as NSAIDS, exert gastrointestinal side effects, suggesting that additional approaches are needed to manage CRC (3, 4). Use of natural products with limited or no toxicity is one such approach to prevent, suppress or reverse the carcinogenesis process (5). In this regard, several studies have indicated that one-third of all cancer deaths in US could be prevented through diet modification and that high consumption of fruits and vegetables or their bioactive components could significantly decrease CRC (5-7). Grape seed extract (GSE) is one such natural agent, rich in proanthocyanidins, which has shown cancer chemopreventive and anti-cancer efficacy in various pre-clinical cancer models including CRC (6, 8, 9). Importantly, clinical studies have shown that active components of GSE are bioavailable and well tolerated in humans (10). However, to our knowledge, GSE has not been examined in mouse model of sporadic CRC. Considering that the sporadic CRC patient population represents the largest clinical population of diagnosed CRC, we aimed to evaluate GSE efficacy against a chemical carcinogen azoxymethane (AOM)-induced colon tumorigenesis in A/J mouse model that mimics generation of sporadic neoplastic lesions as observed in the human colon (11). Furthermore, we also conducted mechanistic studies interlinking miRNA expression with cytokine signaling and inflammation in overall efficacy of GSE against colon tumorigenesis.

Materials and Methods

Reagents

GSE-standardized preparation was a gift from Kikkoman Corp. (Nado City, Japan). As reported earlier (12), the analyzed composition of GSE is 89.3% procyanidins, 6.6% monomeric flavanols, 2.24% moisture content, 1.06% of protein, and 0.8% of ash. AOM was purchased from Sigma (St. Louis, MO) and dissolved in saline. Primary antibodies include, anti- PCNA from Dako; anti-iNOS, anti-VEGF, anti-Ago2 from Abcam (Cambridge, MA); anti-COX-2, anti-C-myc, anti- β -catenin from Santa Cruz Biotechnology (Dallas, TX); anti-phospho-ERK1/2 and anti-NF κ B/p65 from Cell Signaling (Beverly, MA); and anti-mouse and anti-rabbit horseradish peroxidase (HRP) secondary antibodies from Invitrogen (Grand Island, NY) and Cell Signaling, respectively. Mouse cytokine antibody array was from RayBiotech (Norcross, GA). miRNA was isolated using Qiagen miRNeasy Kit, amplified by Qiagen RT² miRNA qPCR kit and quantified using miRNA Cancer PCR array (Qiagen, Valencia, CA).

Animals and treatments

Animal experiment was done under institutional guidelines using approved IACUC protocol. Animals were maintained under standard conditions with free access to water and food. GSE was mixed in AIN-76A powder diet (Dyets Inc.) at 0.25% and 0.5% (w/w). 5 week old male A/J mice (from Jackson Laboratory) were fed AIN-76A powder diet for two weeks (to acclimatize them to new diet) and then divided into 5 groups: [1] negative control group (n=20) on AIN-76 diet; [2] positive control group (AOM, n=35), injected with 5 mg/kg AOM *i.p.* once a week for 6 weeks, and on AIN-76A diet; [3] AOM+0.25% GSE group (n=35), GSE supplemented diet was started 2 weeks post last AOM injection and continued for 18 weeks (n=25) or 28 weeks (n=10); [4] AOM+0.5% GSE group (n=35), GSE

supplemented diet was started 2 weeks post last AOM injection and continued for 18 weeks (n=25) or 28 weeks (n=10); and [5] 0.5% GSE group, GSE supplemented diet was started at 5 weeks of mice age and continued for remainder of study. The selection of two GSE doses for current study was based on our published studies wherein these GSE doses showed a dose-dependent chemopreventive effect against AOM-induced aberrant crypt foci formation in F344 rats and strong efficacy against small intestine tumorigenesis in APC min/+ mouse models (8, 9). Similarly, the selection of AOM-induced colon tumorigenesis experimental protocol in A/J mice in present study was based on our and others recent studies showing measurable to strong colon tumor numbers for agent chemopreventive efficacy studies (5, 13). Body weight and diet consumption were recorded weekly. At the end of the study, at 33 and 43 weeks of age, mice were sacrificed, entire colon excised starting from ileocecal junction to anal verge and cut open longitudinally along main axis and gently flushed with ice-cold PBS, divided in to three equal sections (proximal, medial and distal), tumors counted, and tumor diameters measured with digital calipers under dissecting microscope. Colon tissues and/or tumors were either fixed flat in formalin and embedded in paraffin, snap-frozen in liquid nitrogen, or stored in Qiagen RNA*later* (Valencia, CA).

Anatomical Magnetic Resonance Imaging (MRI)

Anatomical gadolinium enhanced T1-weighted MRI was also employed to non-invasively assess colon tumor progression in mice. Bruker multi slice multi echo (MSME) T1-scans were performed at a Bruker 4.7 Tesla PharmaScan (Bruker Medical, Billerica, MA) following a bolus injection of 0.1 mmol/kg MultiHance via a tail catheter on anesthetized mice (2% isoflurane). A mouse volume transmitter/receiver coil (36 mm diameter) was used for all MRI studies using flowing parameters: FOV=4cm, slice thickness 1 mm, number of slices 16 (coronal) and 40 (axial), TR/TE=725/11 ms, number of averages 2, matrix size 256×256, flip angle 180. Total acquisition time was 6.5 min for each plane. All imaging acquisition and analysis was performed using Bruker ParaVision software (at the Animal Imaging Shared Resources, University of Colorado Anschutz Medical Campus).

Mouse cytokine expression

Tissue lysates of colonic mucosa with tumors from randomly selected animals in different groups were applied to Mouse Cytokine Antibody Array. Expression of various cytokine molecules was analyzed in duplicate on the membranes, which were scanned and quantified by ImageJ, and densitometric data analyzed using antibody array analysis tool.

Mouse miRNA expression

miRNA isolation was done utilizing Qiagen miRNeasy Kit, starting with 20mg of mouse colonic mucosa with tumors. Isolated miRNA was used for miRNA arrays using Qiagen RT² miRNA qPCR kit utilizing Applied Biosciences Fast-Real time PCR 7500. Replicates were performed and the average ΔC_t value of each miRNA assay was calculated for each group. The $\Delta\Delta C_t$ was calculated for each miRNA between = ΔC_t (AOM+0.5% GSE) – ΔC_t (AOM), then the fold-change was calculated for each miRNA.

Immunohistochemistry (IHC) and statistical analyses

Paraffin-embedded sections (5 μ m) of distal colon were subjected to standard IHC procedures described previously (8). Dilutions of primary anti-bodies used were anti-PCNA (1:250), anti-iNOS (1:100), anti-COX-2 (1:50), anti-phospho-ERK1/2 (1:100), anti-Ago2 (1:100), anti- β -catenin (1:50), anti-NF κ B/p65 (1:50), anti-VEGF (1:100) and anti-c-myc (1:25). Negative staining controls were used for each protein. Apoptotic cells were detected by DeadEnd Colorimetric TUNEL system (Promega) (8). Microscopic analyses were performed using Zeiss Axioscope 2 microscope; photomicrographs captured by Carl Zeiss

AxioCam MrC5 camera with Axiovision Rel 4.5 software. Quantification of IHC data includes counts from both colonic mucosa and tumor staining and is shown as mean \pm standard error mean (SEM) from 10 fields/section in each group. Statistically significant difference between AOM and AOM+GSE groups was analysed for tumor multiplicity, tumor size and protein expression using one-way ANOVA (Sigma Stat 2.03, Jandel Scientific, San Rafael, CA). *P* values of < 0.05 were considered significant.

Results

Dietary GSE feeding suppresses AOM-induced colon tumorigenesis (MRI-study)

GSE feeding did not show considerable difference in diet consumption and body weight gain profiles between AOM and AOM+GSE-fed mice during entire study (data not shown). Real time assessment of colon tumor formation was performed in negative control, AOM and AOM+0.5% GSE mice at 32 weeks of age using CE-MRI (Fig 1A). We did not detect any tumors/other lesions or abnormalities in negative control mice, which were further confirmed upon necropsy (performed one week post-MRI at 33 weeks of mice age) (Fig. 1A, left panel). In AOM group, 6 tumors were detected on gadolinium enhanced T1-MRI images and 12 tumors were eventually found upon necropsy (Fig. 1A, middle panel). Mice in AOM+0.50% GSE group showed 3 tumors on MRI while necropsy identified 4 tumors (Fig. 1A, right panel). Comparing the number of tumors between AOM and AOM+0.5% GSE groups, GSE treatment resulted in 50 to 67% inhibition as identified by gadolinium enhanced T1-MRI and necropsy, respectively.

Dietary GSE feeding suppresses AOM-induced tumorigenesis in both colon and small intestine

Figure 1B summarizes the effect of GSE feeding on AOM-induced tumor formation in both colon and small intestine following necropsy. Whereas AOM group showed 8.56 ± 0.58 colon tumors/mouse at 33 weeks of age, GSE treatment post-AOM exposure significantly reduced colon tumorigenesis in a dose-dependent manner; specifically, there was a 46% ($P < 0.001$) and 55% ($P < 0.001$) inhibition in the number of colon tumors in AOM+0.25% GSE and AOM+0.5% GSE groups (Fig. 1B), respectively. Significant inhibition in colon tumorigenesis by GSE feeding was also observed at 43 weeks of mouse age; however, the two doses showed comparable efficacy (Fig. 1B). GSE feeding also significantly decreased the number of small intestine tumors compared to AOM group (Fig. 1B); however, again there was no GSE-dose-response effect.

Since tumor incidence is greater in distal region of the colon in AOM mouse model, GSE effect on tumor formation in different regions of the colon was also analyzed. At 33 weeks of age, AOM group showed 2.97 ± 0.3 colon tumors in the distal region/mouse, while AOM +0.5% GSE group had 1.66 ± 0.2 tumors, indicating a 44% ($P < 0.001$) reduction in tumor formation in the distal region by GSE feeding (data not shown). This trend was also observed in other regions (proximal and medial) of the colon and also at 43 weeks of mouse age (data not shown); 0.25% and 0.5% GSE doses showed comparable efficacy. Additional analysis of colon tumorigenesis study data showed that GSE-feeding also reduces the overall tumor size (Fig. 1C). Importantly, while there was a significant dose-dependent decrease in the number of tumors in the size range of 2-3 mm, there were absolutely no tumors larger than 3mm in AOM+GSE-fed groups compared to AOM alone (Fig. 1C).

Dietary GSE feeding decreases proliferation but induces apoptosis in its efficacy against AOM-induced colon tumorigenesis

CRC growth and progression to advanced stages is associated with enhanced cell proliferation and evasion of apoptosis (11), and therefore the agents which could inhibit

proliferation and induce apoptosis could play an important role in controlling CRC growth and progression (5). Since we found strong efficacy of GSE in preventing AOM-induced colon tumorigenesis, tissue samples were next analyzed for proliferation and apoptotic indices. Qualitative examination of PCNA-stained sections showed a decrease in PCNA-positive cells in AOM+GSE-fed groups compared to AOM alone (Fig. 2A). Further quantification showed $17\pm2\%$ PCNA-positive cells in AOM+0.25% and AOM+0.5% GSE-fed groups of mice compared to $47\pm5\%$, in AOM alone (Fig. 2A), accounting for 65% ($P<0.001$) decrease in proliferation. Regarding *in vivo* apoptosis, GSE feeding on AOM-induced colon tumorigenesis, qualitative microscopic examination showed increased number of TUNEL-positive cells in AOM+GSE-fed groups compared to AOM alone (Fig. 2B). The number of apoptotic cells were ~5% (Fig. 2B, $P<0.001$) in both AOM+GSE-fed groups compared to $1.7\pm0.43\%$ in AOM alone, accounting for a 3-fold ($P<0.001$) increase (Fig. 2B).

Dietary GSE feeding alters cytokine and miRNA expression profiles as well as miRNA processing machinery in its efficacy against AOM-induced colon tumorigenesis

The mixture of host-derived cytokines produced in the tumor microenvironment plays an important role in cancer progression (14) where cancer cells employ cytokines to promote growth, diminish apoptosis, and stimulate both invasion and metastasis (14). Thus, management of cytokine equilibrium could be an important strategy for both prevention and treatment of various malignancies including CRC (14). To examine whether GSE efficacy against AOM-induced colon tumorigenesis involves altered expression of various cytokines, we used inflammatory cytokine antibody array analysis on colonic mucosa with tumors from AOM and AOM+0.5% GSE groups (Fig. 3A). Our results indicated that GSE feeding causes an alteration in the expression of various cytokines/interleukins involved in innate immunity, proliferation and apoptotic cell death. Specifically, GSE up regulated the levels of B-lymphocyte chemo attractant (BLC ~8-fold), granulocyte macrophage-colony stimulating factor (GM-CSF ~10-fold), chemokine CCL1 (I-309 ~9-fold), interleukin (IL)-1 α (~10-fold), IL-23 (~20-fold) and M-CSF (~9-fold), but down regulated IL-1ra (~26-fold), IL-2 (~9-fold) and IL-27 (~8-fold) levels compared to AOM alone (Fig. 3A).

miRNAs are small non-coding RNAs which are implicated in cell cycle regulation, cell growth and differentiation, stress response and apoptosis (15). In addition, miRNAs also play an essential role during carcinogenesis and their expression patterns have been now correlated with disease prognosis in cancer patients (15). Furthermore, miRNA knock down or re-expression induces drug sensitivity, impede proliferation, and reduce invasion of cancer cells (15). In view of above summarized critical roles of miRNAs, next we assessed whether their altered expression also contributes to GSE efficacy against AOM-induced colon tumorigenesis. A comparison of miRNA expression profiles of the tissue from AOM and AOM+0.5% GSE groups showed that GSE feeding causes an up regulation of Snord 68 (~6500-fold), miR-19a (~2400-fold), miR-20a (~1000-fold) and miR-let7a (~1200-fold) (Fig. 3B), but down regulates miR-205 (~400-fold), miR-135b (~100-fold), miR-196a (~24-fold), miR-21 (~25-fold), miR-148a (~21-fold) and miR-103 (~9-fold) (Fig. 3B). Furthermore, IHC analysis revealed a ~6.5 fold induction in the level of Ago2, which is involved in miRNA processing (16), in AOM+0.5% GSE group compared to AOM alone, indicating an increased RNA-induced gene silencing in response to GSE feeding (Fig. 3C).

Based on an extensive literature search for the possible role of above identified various cytokines/interleukins and miRNAs with altered expression following GSE treatment and the associated cross-talks among them, we were able to identify a pattern in their modulation as discussed in detail in the discussion section (14, 17, 18).. Specifically, we found that GSE mediates its efficacy against AOM-induced colon tumorigenesis by possibly modulating NF- κ B and its downstream targets related to inflammatory signaling, β catenin signaling,

and MAPK pathway. Accordingly, next we investigated their possible roles in GSE efficacy against AOM-induced colon tumorigenesis.

Dietary GSE feeding inhibits NF-κB activation and decreases expression of associated molecules in its efficacy against AOM-induced colon tumorigenesis

Transcription factor NF-κB mediates the transcription of various genes which are associated with tumor initiation, promotion, progression, metastasis as well as inflammation, including those for COX-2, iNOS and VEGF (19). Additionally, inflammation is associated with CRC development, and chronic inflammation increases CRC risk (20). In addition, experimental and epidemiological evidences indicate an up regulation of COX-2, iNOS and VEGF (downstream target genes of NF-κB) in various malignancies, including human CRC (21). Together, based on this information and our array data analyses suggesting the involvement of NF-κB and its downstream inflammatory molecules in GSE efficacy, IHC analyses were done to examine their expression. Our results showed that GSE feeding indeed interferes with NF-κB activity, as observed by a significant decrease in nuclear expression of NF-κB/p65 in the distal colon/tumor tissues by both GSE doses (Fig. 4A). Next we examined COX-2 and iNOS levels (Fig. 4B & C). AOM alone treated mice showed a significant increase in COX-2 and iNOS immunoreactivity scores [\sim 10 folds ($P<0.001$) and \sim 2.5 folds ($P<0.001$) respectively] in the distal colon/tumor tissues, compared to untreated negative controls. Importantly, mice in the AOM+GSE-fed groups exhibited a significant down regulation of COX-2 and iNOS protein levels in the distal colon/tumor tissues (Fig. 4B & C). Similarly, a decrease in VEGF immunoreactivity scores (Fig. 4D) was also observed in the distal colon/tumor tissues from the mice in AOM+GSE-fed groups compared to AOM alone.

Dietary GSE feeding modulates β-catenin and MAPK pathways in its efficacy against AOM-induced colon tumorigenesis

Our array data analyses also suggested a possible involvement of β-catenin and MAPK signaling in GSE efficacy against AOM-induced colon tumorigenesis, and accordingly, next we focused on these two pathways. β-catenin is important in the development of CRC and inappropriate stabilization, translocation and activation of β-catenin occur in sporadic and familial CRC resulting in downstream modulation of oncogenic target genes such as *c-myc* and *VEGF*(22). IHC results for β-catenin staining revealed a significant dose-dependent reduction ($P<0.001$) in the nuclear expression of β-catenin in the distal colon/tumor tissues of AOM+GSE-fed groups compared to AOM alone (Fig. 5A). Following the above results and further examining the downstream β-catenin pathway targets, we assessed the expression of C-myc (22). The quantification of IHC staining for C-myc in distal colon/tumor tissues revealed a significant ($P<0.001$) dose-dependent reduction in AOM+GSE groups compared to AOM alone (Fig. 5B). The RAS-RAF-MEK-MAPK signaling cascade plays an important role in tumorigenesis including CRC (23), and accordingly we also investigated the role of this pathway in GSE efficacy against AOM-induced colon tumorigenesis by assessing the expression of extracellular signal-regulated kinase 1/2 (ERK1/2), which is phosphorylated in response to RAS activation (23). Microscopic examination of distal colon/tumor tissue sections from all groups revealed a significant reduction (94-97%, $P<0.001$) in the phosphorylation of ERK1/2 (Fig. 5C) in AOM+GSE-fed groups compared to AOM alone.

Discussion

This is the first study reporting that long-term dietary feeding of GSE (0.25% and 0.5% w/w in AIN-76A diet) for 18 and 28 weeks following exposure to AOM results in a significant decrease in AOM-induced colon tumor multiplicity. More importantly, GSE feeding caused

a significant reduction in colon tumor size in a dose-dependent manner. Furthermore, GSE feeding did not show any effect on food consumption and body weight-gain profiles, which is consistent with previous anti-cancer efficacy studies with GSE in other cancer models (6). In the present study, we also established feasibility of non-invasive real-time examination of colon lesions by gadolinium-enhanced MRI, which allowed the visualization of colon tumors in AOM mouse model with 75-81% sensitivity. This, somewhat low, sensitivity of MRI (as compared to necropsy results) can be attributed to non-optimal experimental conditions during tumor visualization (such as small size lesions and bowel movements), which could possibly be improved in future by altering image contrast as reported for other studies (24). Biomarker analyses in colonic mucosa with tumors indicated that GSE feeding decreases proliferation but induces apoptosis in its chemopreventive efficacy. We also focused our efforts on identifying the targets and pathways modulated by GSE in its colon cancer chemopreventive efficacy by utilizing cytokine and miRNA arrays. Our results and their analyses showed that a wide number of cytokines/ILs and miRNAs were significantly modulated by GSE which were associated with alterations in NF- κ B, β -catenin and MAPK signaling, suggesting that inflammation, proliferation and apoptosis are targeted by GSE in its chemopreventive efficacy. However, unlike previous studies with GSE by us and others showing a dose-dependent cancer chemopreventive and anti-cancer efficacy in various cancer models including AOM-induced ACF in rats (8), in present study we observed comparable efficacy of GSE on colon tumor numbers and most of the associated mechanistic pathways. However, GSE did affect colon tumor sizes as well as β -catenin and C-myc expression in colon tumor tissues in a dose-response manner. Together, these findings suggest that possibly a lower dose of GSE is optimum for its efficacy in AOM-induced colon tumorigenesis in A/J mice, and that additional proliferation markers should be examined in future to further support β -catenin and C-myc findings.

Further analysis of array data showed that GSE decreases IL-2, which is an important finding because activation of NF- κ B, a transcription factor associated with inflammation, leads to IL-2 production (25). GSE also significantly down regulated the levels of IL-27 and IL-1 α , which are known to modify NF- κ B signaling (26-28). Similarly, miRNA array analysis showed that GSE up regulates miR-19a, which is linked to NF- κ B regulation (29). miR-20a is known to inhibit HIF-1 α pathway, which plays a major role in the survival of cancer cells in tumor microenvironment; importantly, GSE up regulated miR-20a suggesting its activity in inhibiting HIF-1 α pathway and its downstream target VEGF (30, 31). Similarly, miRNA array results showed that GSE causes a dramatic down regulation of miR-205, which targets VEGF (32) that is also transcriptionally regulated by NF- κ B. Consistent with these observations, our results showed that GSE decreases the expression of nuclear NF- κ B p65 subunit as well as those of COX-2, iNOS and VEGF. These results are important as over expression of pro-inflammatory molecules, such as iNOS and COX-2, is observed in AOM-induced CRC and selective COX-2 inhibitors have been shown to prevent disease progression (33, 34). In addition, decreased expression of the pro-angiogenic factor VEGF suggests that GSE might also interfere in tumor angiogenesis; a strong dose-dependent decrease in colon tumor size by GSE supports this notion. Together, these results suggested that GSE exerts its efficacy against colon tumorigenesis at least in part by modulating NF- κ B signaling and its downstream transcriptional targets COX-2, iNOS and VEGF, which are implicated in inflammation, tumor promotion, progression and metastasis of CRC (19, 35, 36).

β -catenin signaling is extensively studied for its critical role in human CRC growth and progression (22), suggesting that the agents targeting this pathway would be useful in CRC control. In our study, we found that GSE causes an increase in M-CSF, which is linked to β -catenin signaling (37). In addition, GSE also significantly decreased miR-135b, which is also linked to β -catenin pathway (38). Moreover, GSE up regulated let-7a, which is

implicated in inhibiting the expression of the *c-myc* oncogene, a downstream target of β -catenin (39). Consistent with these results, GSE significantly down regulated β -catenin protein expression, which was also associated with the decreased expression of its downstream target C-myc (22), suggesting their possible role in GSE efficacy against colon tumorigenesis.

Cytokine/IL array findings also showed up regulation of BLC, CCL1/I-309 and IL-1 α , but down regulation of IL-1rc and IL-27 by GSE; all these molecules are involved in regulating the MAPK pathway (40-43). Furthermore, in miRNA array analysis, GSE showed an up regulation of let-7a which is known to inhibit MAPK pathway (44). We also found that GSE decreases miR-205, which is up regulated in some malignancies and known to interact with both MAPK and NOTCH pathways (45). Notably, MAPK signaling cascade is known to play an important role in tumorigenesis by modulating cell growth, differentiation, proliferation, apoptosis, and migration (23). GSE also decreased miR-103, which is involved in oncogenic *KRAS* signaling and is up regulated in CRC cells (46). Our IHC results clearly showed that GSE causes a strong decrease in MAPK/ERK1/2 phosphorylation which is consistent with our cytokine/IL and miRNA array profiles. Together, these results suggested that GSE exerts its efficacy against colon tumorigenesis at least in part by also modulating KRAS-MAPK signaling.

In addition to the miRNAs described above and their association with signaling pathways, GSE also modulated the expression of several additional miRNAs, which are implicated in CRC. For example, GSE down regulated miR-135b that is up regulated in CRC tissue compared to the normal surrounding tissue and has been specifically shown to target the APC gene involved in CRC (47, 48). Similarly, GSE decreased miR-196a, the high-levels of this miRNA exert a pro-oncogenic effect in CRC cells (49). Likewise, the ability of GSE to decrease miR-21 is of clinical significance, because its increased levels correlate with increased stage of clinical CRC (47, 50). Importantly, in this study, we also observed predominate global up regulation of miRNAs by GSE, coupled with down regulation of oncogenic miRNAs and up-regulation of tumor suppressive miRNAs. Accordingly, we also investigated a key protein involved in miRNA homeostasis (16), namely Ago2, which binds to the mRNA and represses translation or translocation. Colon tissue analysis revealed significant up regulation of Ago2 protein in colons of AOM+GSE-fed groups, which further supports our miRNA array results. Together, this is the first study showing alteration in miRNAs expression and cytokine signaling by GSE in its chemopreventive efficacy against AOM-induced colon tumorigenesis in A/J mouse sporadic CRC model.

Acknowledgments

Grant support: This work was supported by NIH R01 AT003623; NCI Cancer Center P30 CA046934; NCRR CTSA UL1 RR025780.

References

1. American Cancer Society: Cancer Facts and Figures 2012.
2. Brethauer M. Evidence for colorectal cancer screening. Best Pract Res Clin Gastroenterol. 2010; 24:417–25. [PubMed: 20833346]
3. Half E, Arber N. Colon cancer: preventive agents and the present status of chemoprevention. Expert Opin Pharmacother. 2009; 10:211–9. [PubMed: 19236194]
4. Lanas A, Fernandez A. NSAIDs and the colon. Curr Opin Gastroenterol. 2009; 25:44–9. [PubMed: 19114773]
5. Rajamanickam S, Agarwal R. Natural products and colon cancer: current status and future prospects. Drug Dev Res. 2008; 69:460–71. [PubMed: 19884979]

6. Kaur M, Agarwal C, Agarwal R. Anticancer and cancer chemopreventive potential of grape seed extract and other grape-based products. *The Journal of nutrition*. 2009; 139:1806S–12S. [PubMed: 19640973]
7. Kelloff GJ, Boone CW, Crowell JA, Nayfield SG, Hawk E, Malone WF, et al. Risk biomarkers and current strategies for cancer chemoprevention. *J Cell Biochem Suppl*. 1996; 25:1–14. [PubMed: 9027592]
8. Velmurugan B, Singh RP, Agarwal R, Agarwal C. Dietary-feeding of grape seed extract prevents azoxymethane-induced colonic aberrant crypt foci formation in fischer 344 rats. *Molecular carcinogenesis*. 2010; 49:641–52. [PubMed: 20564341]
9. Velmurugan B, Singh RP, Kaul N, Agarwal R, Agarwal C. Dietary feeding of grape seed extract prevents intestinal tumorigenesis in APCmin/+ mice. *Neoplasia*. 2010; 12:95–102. [PubMed: 20072658]
10. Eich, N.; Schneider, E.; Cuomo, J.; Rabovsky, A.; Vita, JA.; Palmisano, J., et al. Bioavailability of epicatechin after consumption of grape seed extract in humans; Experimental Biology Meeting; Washington, DC. abstr 2012
11. Rosenberg DW, Giardina C, Tanaka T. Mouse models for the study of colon carcinogenesis. *Carcinogenesis*. 2009; 30:183–96. [PubMed: 19037092]
12. Veluri R, Singh RP, Liu Z, Thompson JA, Agarwal R, Agarwal C. Fractionation of grape seed extract and identification of gallic acid as one of the major active constituents causing growth inhibition and apoptotic death of DU145 human prostate carcinoma cells. *Carcinogenesis*. 2006; 27:1445–53. [PubMed: 16474170]
13. Ravichandran K, Velmurugan B, Gu M, Singh RP, Agarwal R. Inhibitory effect of silibinin against azoxymethane-induced colon tumorigenesis in A/J mice. *Clinical cancer research: an official journal of the American Association for Cancer Research*. 2010; 16:4595–606. [PubMed: 20823143]
14. Dranoff G. Cytokines in cancer pathogenesis and cancer therapy. *Nature reviews Cancer*. 2004; 4:11–22.
15. Croce CM. Causes and consequences of microRNA dysregulation in cancer. *Nat Rev Genet*. 2009; 10:704–14. [PubMed: 19763153]
16. Taliaferro JM, Aspden JL, Bradley T, Marwha D, Blanchette M, Rio DC. Two new and distinct roles for Drosophila Argonaute-2 in the nucleus: alternative pre-mRNA splicing and transcriptional repression. *Genes & development*. 2013
17. Faber C, Kirchner T, Hlubek F. The impact of microRNAs on colorectal cancer. *Virchows Arch*. 2009; 454:359–67. [PubMed: 19288129]
18. Slaby O, Svoboda M, Michalek J, Vyzula R. MicroRNAs in colorectal cancer: translation of molecular biology into clinical application. *Mol Cancer*. 2009; 8:102. [PubMed: 19912656]
19. Greten FR, Karin M. The IKK/NF-kappaB activation pathway-a target for prevention and treatment of cancer. *Cancer Lett*. 2004; 206:193–9. [PubMed: 15013524]
20. Danese S, Mantovani A. Inflammatory bowel disease and intestinal cancer: a paradigm of the Yin-Yang interplay between inflammation and cancer. *Oncogene*. 2010; 29:3313–23. [PubMed: 20400974]
21. Ohta T, Takahashi M, Ochiai A. Increased protein expression of both inducible nitric oxide synthase and cyclooxygenase-2 in human colon cancers. *Cancer Lett*. 2006; 239:246–53. [PubMed: 16216410]
22. Barker N, Clevers H. Mining the Wnt pathway for cancer therapeutics. *Nat Rev Drug Discov*. 2006; 5:997–1014. [PubMed: 17139285]
23. Santarpia L, Lippman SM, El-Naggar AK. Targeting the MAPK-RAS-RAF signaling pathway in cancer therapy. *Expert Opin Ther Targets*. 2012; 16:103–19. [PubMed: 22239440]
24. Young MR, Ileva LV, Bernardo M, Riffle LA, Jones YL, Kim YS, et al. Monitoring of tumor promotion and progression in a mouse model of inflammation-induced colon cancer with magnetic resonance colonography. *Neoplasia*. 2009; 11:237–46. 1p following 46. [PubMed: 19242605]
25. Arima N, Kuziel WA, Grdina TA, Greene WC. IL-2-induced signal transduction involves the activation of nuclear NF-kappa B expression. *J Immunol*. 1992; 149:83–91. [PubMed: 1607664]

26. Guzzo C, Ayer A, Basta S, Banfield BW, Gee K. IL-27 enhances LPS-induced proinflammatory cytokine production via upregulation of TLR4 expression and signaling in human monocytes. *J Immunol.* 2012; 188:864–73. [PubMed: 22156348]
27. Guzzo C, Hopman WM, Che Mat NF, Wobeser W, Gee K. IL-27-induced gene expression is downregulated in HIV-infected subjects. *PLoS one.* 2012; 7:e45706. [PubMed: 23049843]
28. Hartupee J, Li X, Hamilton T. Interleukin 1alpha-induced NF κ B activation and chemokine mRNA stabilization diverge at IRAK1. *The Journal of biological chemistry.* 2008; 283:15689–93. [PubMed: 18411265]
29. Gantier MP, Stundem HJ, McCoy CE, Behlke MA, Wang D, Kaparakis-Liaskos M, et al. A miR-19 regulon that controls NF- κ B signaling. *Nucleic Acids Res.* 2012; 40:8048–58. [PubMed: 22684508]
30. Kang SG, Lee WH, Lee YH, Lee YS, Kim SG. Hypoxia-inducible factor-1alpha inhibition by a pyrrolopyrazine metabolite of oltipraz as a consequence of microRNAs 199a-5p and 20a induction. *Carcinogenesis.* 2012; 33:661–9. [PubMed: 22223846]
31. Semenza GL. Involvement of hypoxia-inducible factor 1 in human cancer. *Intern Med.* 2002; 41:79–83. [PubMed: 11868612]
32. Wu H, Zhu S, Mo YY. Suppression of cell growth and invasion by miR-205 in breast cancer. *Cell Res.* 2009; 19:439–48. [PubMed: 19238171]
33. van der Woude CJ, Kleibeuker JH, Jansen PL, Moshage H. Chronic inflammation, apoptosis and (pre-)malignant lesions in the gastro-intestinal tract. *Apoptosis.* 2004; 9:123–30. [PubMed: 15004509]
34. Rao CV, Indranie C, Simi B, Manning PT, Connor JR, Reddy BS. Chemopreventive properties of a selective inducible nitric oxide synthase inhibitor in colon carcinogenesis, administered alone or in combination with celecoxib, a selective cyclooxygenase-2 inhibitor. *Cancer research.* 2002; 62:165–70. [PubMed: 11782374]
35. Karin M. Nuclear factor- κ B in cancer development and progression. *Nature.* 2006; 441:431–6. [PubMed: 16724054]
36. Pikarsky E, Porat RM, Stein I, Abramovitch R, Amit S, Kasem S, et al. NF- κ B functions as a tumour promoter in inflammation-associated cancer. *Nature.* 2004; 431:461–6. [PubMed: 15329734]
37. Fujita K, Janz S. Attenuation of WNT signaling by DKK-1 and -2 regulates BMP2-induced osteoblast differentiation and expression of OPG, RANKL and M-CSF. *Mol Cancer.* 2007; 6:71. [PubMed: 17971207]
38. Huang K, Zhang JX, Han L, You YP, Jiang T, Pu PY, et al. MicroRNA roles in beta-catenin pathway. *Mol Cancer.* 2010; 9:252. [PubMed: 20858269]
39. Sampson VB, Rong NH, Han J, Yang Q, Aris V, Soteropoulos P, et al. MicroRNA let-7a down-regulates MYC and reverts MYC-induced growth in Burkitt lymphoma cells. *Cancer research.* 2007; 67:9762–70. [PubMed: 17942906]
40. Burkle A, Niedermeier M, Schmitt-Graff A, Wierda WG, Keating MJ, Burger JA. Overexpression of the CXCR5 chemokine receptor, and its ligand, CXCL13 in B-cell chronic lymphocytic leukemia. *Blood.* 2007; 110:3316–25. [PubMed: 17652619]
41. Louahed J, Struyf S, Demoulin JB, Parmentier M, Van Snick J, Van Damme J, et al. CCR8-dependent activation of the RAS/MAPK pathway mediates anti-apoptotic activity of I-309/CCL1 and vMIP-I. *Eur J Immunol.* 2003; 33:494–501. [PubMed: 12645948]
42. Saklatvala J, Dean J, Finch A. Protein kinase cascades in intracellular signalling by interleukin-1 and tumour necrosis factor. *Biochem Soc Symp.* 1999; 64:63–77. [PubMed: 10207621]
43. Foey AD, Parry SL, Williams LM, Feldmann M, Foxwell BM, Brennan FM. Regulation of monocyte IL-10 synthesis by endogenous IL-1 and TNF-alpha: role of the p38 and p42/44 mitogen-activated protein kinases. *J Immunol.* 1998; 160:920–8. [PubMed: 9551930]
44. Johnson SM, Grosshans H, Shingara J, Byrom M, Jarvis R, Cheng A, et al. RAS is regulated by the let-7 microRNA family. *Cell.* 2005; 120:635–47. [PubMed: 15766527]
45. Xie H, Zhao Y, Caramuta S, Larsson C, Lui WO. miR-205 Expression Promotes Cell proliferation and Migration of Human Cervical Cancer Cells. *PLoS one.* 2012; 7:e46990. [PubMed: 23056551]

46. Chen HY, Lin YM, Chung HC, Lang YD, Lin CJ, Huang J, et al. miR-103/107 promote metastasis of colorectal cancer by targeting the metastasis suppressors DAPK and KLF4. *Cancer research*. 2012; 72:3631–41. [PubMed: 22593189]
47. Xu XM, Qian JC, Deng ZL, Cai Z, Tang T, Wang P, et al. Expression of miR-21, miR-31, miR-96 and miR-135b is correlated with the clinical parameters of colorectal cancer. *Oncology letters*. 2012; 4:339–45. [PubMed: 22844381]
48. Nagel R, le Sage C, Diosdado B, van der Waal M, Oude Vrielink JA, Bolijn A, et al. Regulation of the adenomatous polyposis coli gene by the miR-135 family in colorectal cancer. *Cancer research*. 2008; 68:5795–802. [PubMed: 18632633]
49. Schimanski CC, Frerichs K, Rahman F, Berger M, Lang H, Galle PR, et al. High miR-196a levels promote the oncogenic phenotype of colorectal cancer cells. *World J Gastroenterol*. 2009; 15:2089–96. [PubMed: 19418581]
50. Kjaer-Frifeldt S, Hansen TF, Nielsen BS, Joergensen S, Lindebjerg J, Soerensen FB, et al. The prognostic importance of miR-21 in stage II colon cancer: a population-based study. *Br J Cancer*. 2012; 107:1169–74. [PubMed: 23011541]

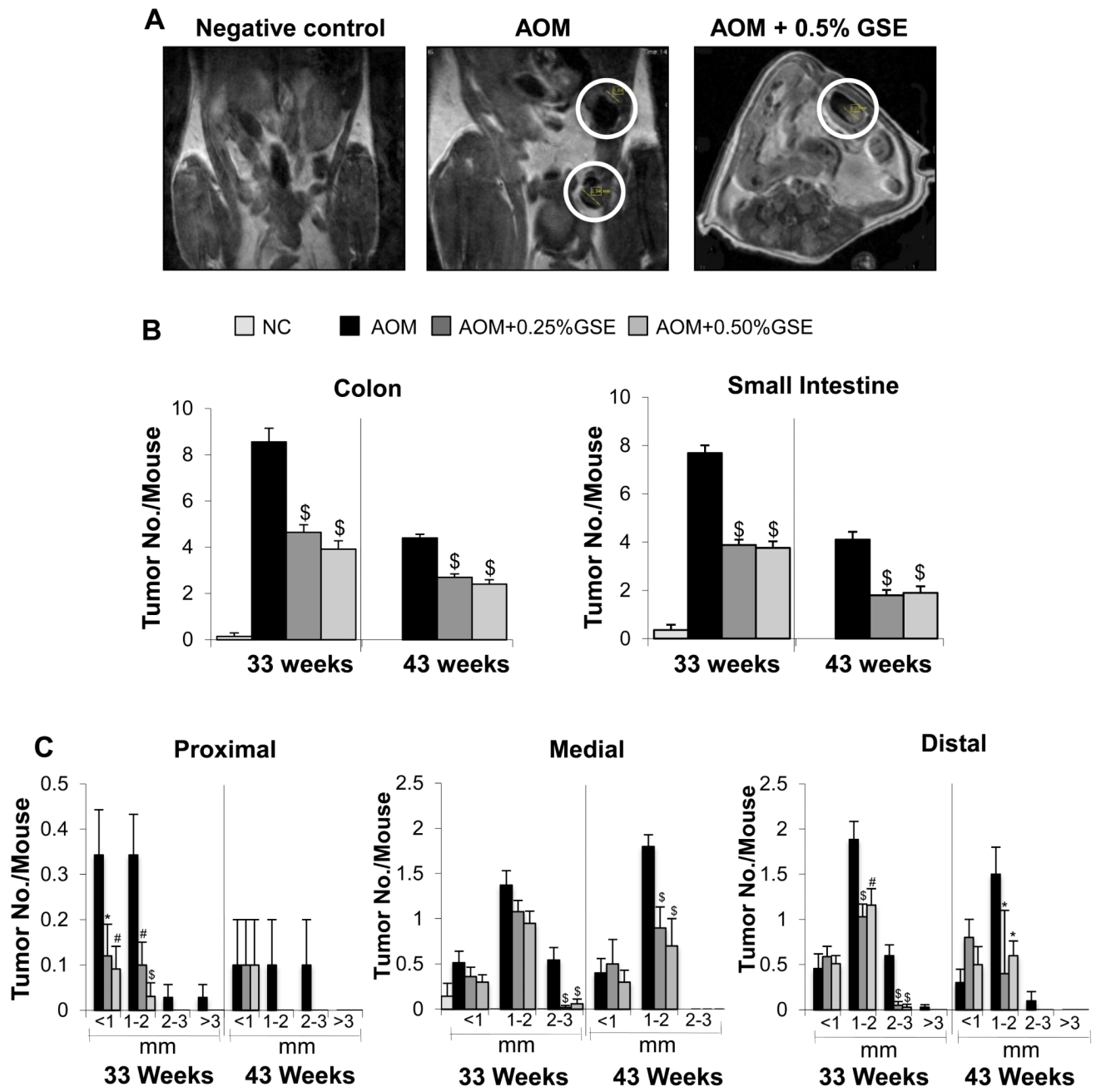


Fig. 1. Chemopreventive efficacy of GSE against AOM-induced colon tumorigenesis in A/J mice
The details of the experimental protocol are outlined in Methods section. (A) Real-time non-invasive assessment of tumor numbers and sizes formed after GSE feeding in AOM exposed A/J mice using non-invasive gadolinium-enhanced T1-MRI. Representative coronal and axial T1-weighted MRI images are presented for untreated negative control (left panel, coronal image), AOM untreated (middle, coronal) and AOM + 0.5% GSE-fed mice (right, axial). Effect of GSE feeding on (B) tumor multiplicity in colon and small intestine and (C) tumor size in colon, in AOM-induced colon tumorigenesis in A/J mice. Columns represent mean \pm SEM (error bars) in each group; * P < 0.05; # P < 0.01; \$ P < 0.001. NC (negative control)

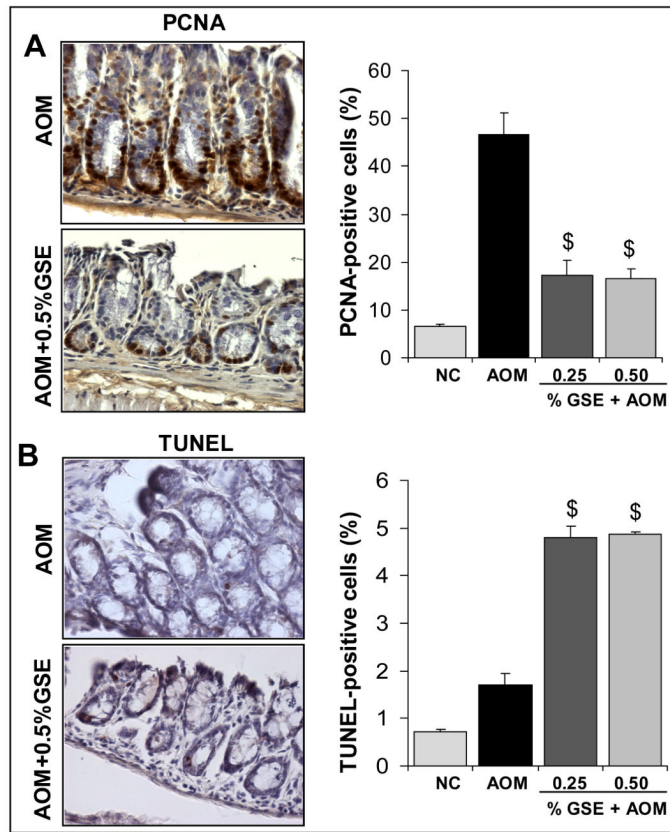


Fig. 2. Dietary GSE feeding decreases proliferation but induces apoptosis in its efficacy against AOM-induced colon tumorigenesis

(A) Anti-proliferative, and (B) pro-apoptotic effects of GSE feeding on colon/tumor tissue from AOM-induced colon tumorigenesis in A/J mice. Immunohistochemical staining for PCNA was based on DAB staining as detailed in “Materials and Methods”. Proliferation index was calculated as the number of positive cells $\times 100$ / total number of cells counted under $\times 400$ magnifications in 10 randomly selected areas in each sample, and shown as mean \pm SEM (error bars) for each group. Apoptosis was analyzed by TUNEL staining in colon/tumor tissues as detailed in “Materials and Methods”. Apoptotic index was calculated as the number of TUNEL-positive cells $\times 100$ / total number of cells counted under $\times 400$ magnifications in 10 randomly selected areas in each sample, and shown as mean \pm SEM (error bars) for each group. \$ P < 0.001. Representative pictographs are depicted at $\times 400$. NC (negative control)

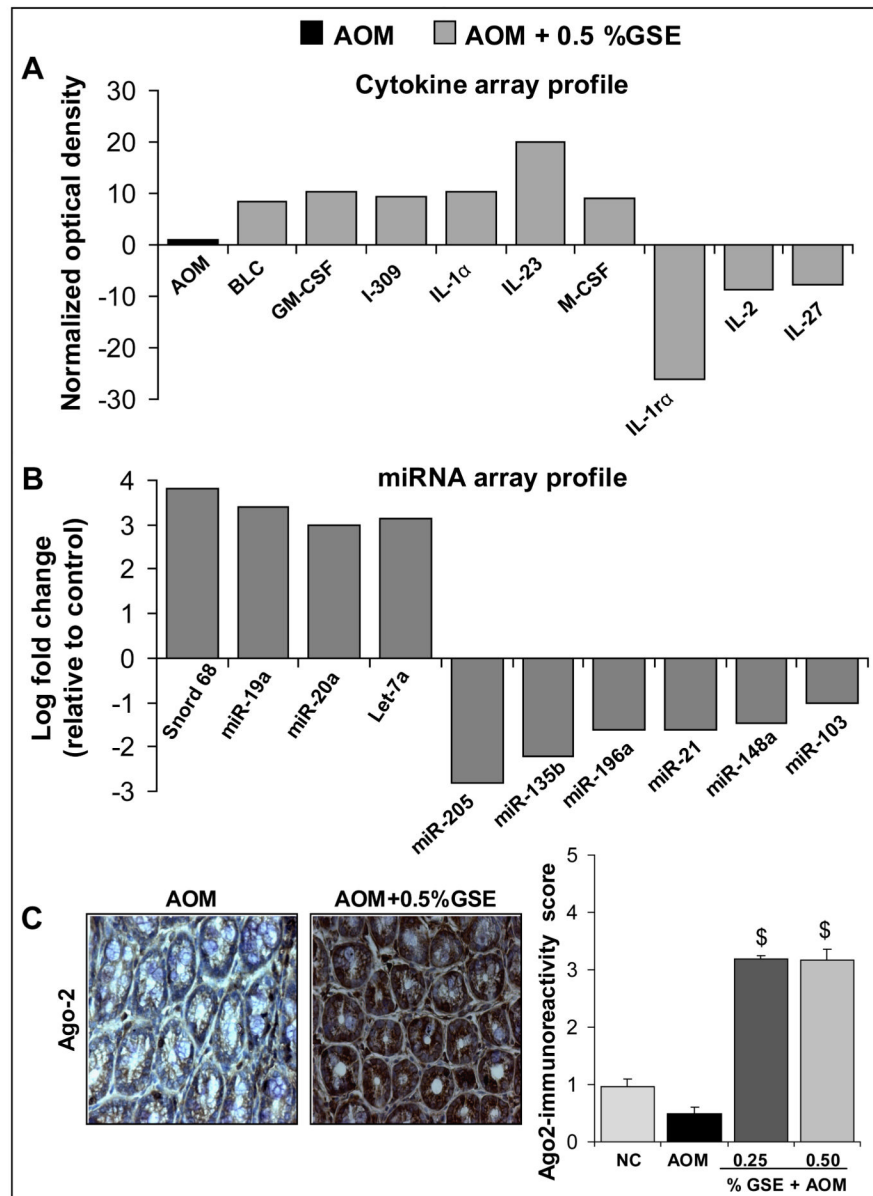


Fig. 3. Dietary GSE feeding alters cytokine and miRNA expression profiles as well as miRNA processing machinery in its efficacy against AOM-induced colon tumorigenesis
 Alteration in (A) cytokine and (B) miRNA expression profiles, and (C) Ago2 expression in colonic mucosa with tumors from AOM-induced colon tumorigenesis in A/J mice. The arrays were done as detailed in “Materials and Methods”. Immunohistochemical staining for Ago2 was based on DAB staining as detailed in “Materials and Methods”. Representative pictographs are depicted at $\times 400$. Immunoreactivity (represented by cytosolic intensity of brown staining) was scored as 0 (no staining), +1 (weak), +2 (moderate), +3 (strong) and +4 (very strong). Columns represent mean \pm SEM (error bars) in each group. \$ P < 0.001. NC (negative control)

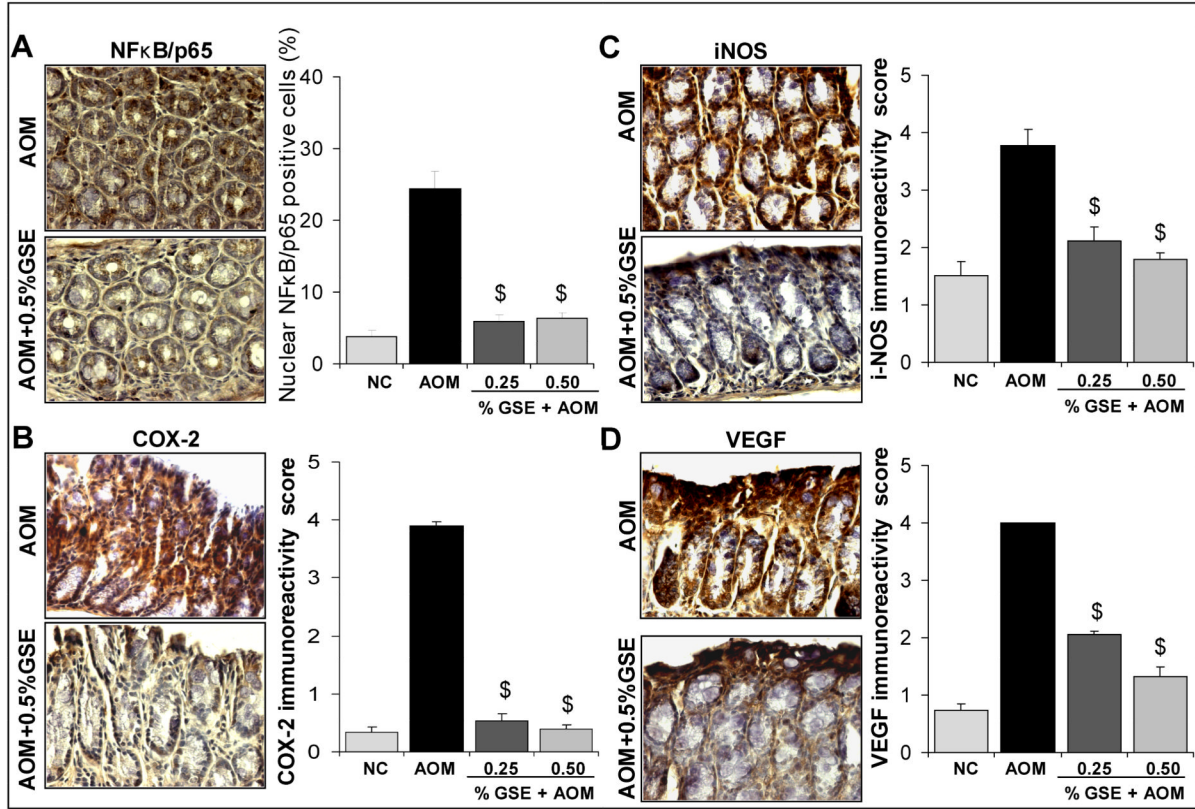


Fig. 4. Dietary GSE feeding inhibits NF-κB activation and decreases associated molecules in its efficacy against AOM-induced colon tumorigenesis

Immunohistochemical staining for (A) NF-κB/p65 (B) COX-2, (C), iNOS, and (D) VEGF was based on DAB staining as detailed in “Materials and Methods”. Representative pictographs are depicted at $\times 400$. Percent positive cells were calculated as number of brown nuclei $\times 100$ / total number of cells counted under $\times 400$ magnifications in 10 randomly selected areas in each sample, and shown as mean \pm SEM (error bars) for each group. Immunoreactivity (represented by cytosolic intensity of brown staining) was scored as 0 (no staining), +1 (weak), +2 (moderate), +3 (strong) and +4 (very strong). Columns represent mean \pm SEM (error bars) in each group. \$ P < 0.001. NC (negative control)

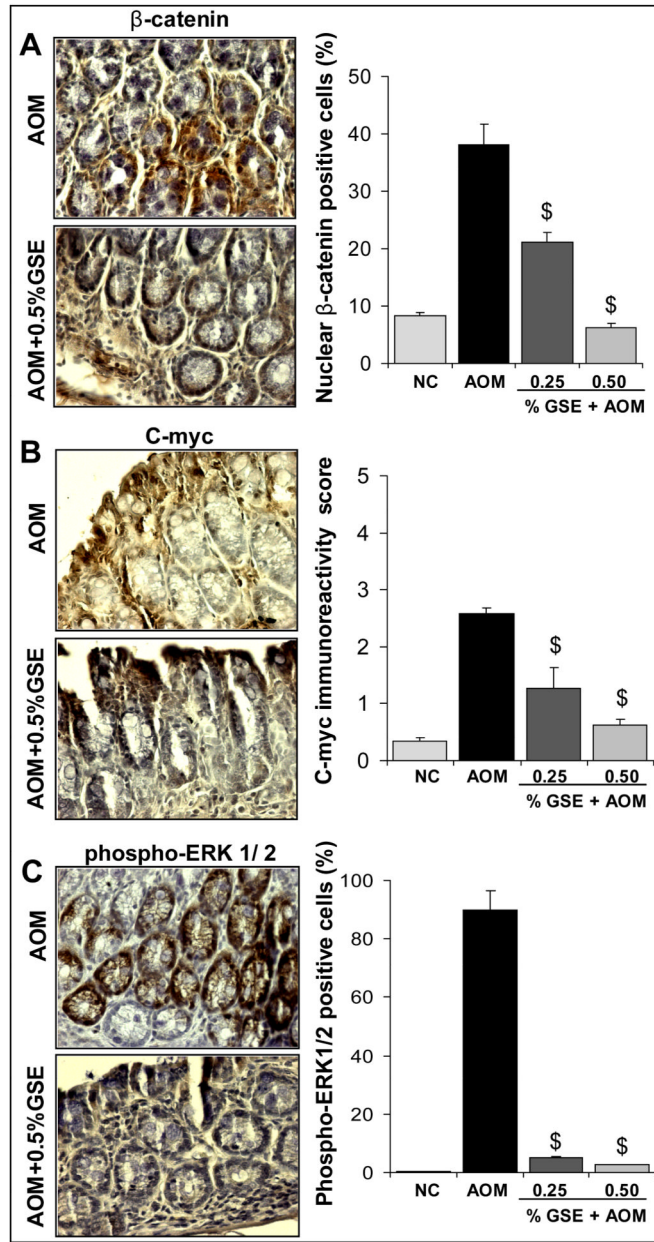


Fig. 5. Dietary GSE feeding modulates β -catenin and MAPK pathways in its efficacy against AOM-induced colon tumorigenesis

Immunohistochemical staining for (A) β -catenin, (B) C-myc, and (C) phospho ERK 1/2 was based on DAB staining as detailed in “Materials and Methods”. Representative DAB-stained tissue specimens from AOM control and AOM+ 0.5% GSE-fed groups showing brown-colored positive cells or cytosolic staining are depicted at $\times 400$ magnifications. Percent positive cells were calculated as number of cells with brown cytoplasmic or nuclei staining $\times 100$ / total number of cells counted under $\times 400$ magnifications in 10 randomly selected areas in each sample, and shown as mean \pm SEM (error bars) for each group.

Immunoreactivity (represented by intensity of brown staining) was scored as 0 (no staining), +1 (weak), +2 (moderate), +3 (strong) and +4 (very strong). Error bars indicate \pm SEM, \$ P < 0.001. NC (negative control).